© APR 2019 | IRE Journals | Volume 2 Issue 10 | ISSN: 2456-8880
DOI: https://doi.org/10.64388/IREV2I10-1722671

Repeated-Load Performance of Concrete Produced with Locally Sourced Aggregates for Road and Drainage Structures

OLADIMEJI BASIT ALAKA[1*], RIDWAN TIAMIYU[2]
[1]*Osun State University, Osogbo, Nigeria*
[2]*University of Ilorin, Ilorin, Nigeria*
**Corresponding author: Oladimeji Basit Alaka*

***Abstract-** Concrete for Nigerian road and drainage structures is produced from whatever coarse aggregate lies within economic haulage distance, and its mechanical quality varies widely between quarries. The static consequences are documented; the fatigue consequences are not, and limited published work relates Nigerian aggregate source to fatigue performance. This research asks how much design life is at stake. We tested 180 flexural fatigue specimens on commercial crushed granite, uncrushed river gravel and artisanal crushed granite, and analyzed the results with a stress-life regression, a two-parameter Weibull description of life scatter and a secant-modulus degradation model. The consequence is large and it inverts the ranking that mean testing would give. At a design stress ratio of 0.65, river gravel costs a factor of 7.47 in mean fatigue life and 18.08 in characteristic life at five percent failure probability; artisanal granite costs 3.48 on the mean but 22.09 on the characteristic basis, the worse material for design despite the better average. Conventional acceptance testing would miss this: across three materials whose characteristic lives differ by more than a factor of twenty, an analysis of variance on 28-day compressive strength returns p=0.051. We recommend that aggregate acceptance for repeatedly loaded concrete constrain the dispersion of the supply, and that source approval be granted per quarry rather than per rock type.*

***Keywords:** concrete fatigue, coarse aggregate variability, stress-life relationship, weibull distribution, rigid pavement, drainage structures, nigeria*

I. INTRODUCTION

Testing rock from eight quarries around Ibadan against the aggregate test suite in BS 812, Ajagbe et al. (2015) found that only five of twelve resulting concrete mixtures reached the 25 N/mm^2 minimum normally required of load-bearing structural members. That single result frames the problem this paper addresses. Concrete carries a large share of Nigeria's road and drainage infrastructure, in rigid pavement sections, box culverts, lined channels, bridge approach slabs and kerbing, and in almost every case the coarse aggregate is whatever can be obtained locally: crushed granite from a commercial quarry, dredged river gravel, or crushed rock from one of the many small-scale operations that supply a local market without formal quality control.

Those materials are not equivalent, and the difference is not marginal. Sampling gravel from four pits across Ogun and Oyo States, Bamigboye et al. (2018) recorded 28-day compressive strengths ranging from 13.5 to 25.3 N/mm^2 for a nominally identical 1:2:4 mix, a near two-fold spread attributable to source alone. Nduka et al. (2018) found quarry-crushed granite outperforming unwashed local river gravel by between 36 and 84 percent in compressive strength across curing ages, and attributed the deficit to silt, clay and organic contamination. The evidence that Nigerian aggregate supply is variable, and that the variability propagates into concrete strength, is substantial and specific.

What that evidence does not address is repeated loading. Every study cited above reports monotonic strength at 7, 14, 21 or 28 days, occasionally with a splitting tensile or flexural result. Yet the structures the concrete goes into do not fail under a single application of load. A pavement slab, a culvert top slab and a drainage channel invert are loaded, unloaded and reloaded with every axle that passes, and for rigid pavement the governing limit state is flexural fatigue cracking rather than static rupture (Packard and Tayabji 1984; Plei and Tayabji 2012). The design question is not whether the concrete can carry the axle once. It is how many times.

The international fatigue literature answers that question thoroughly, but for other materials. The stress-life relations that underpin practice, from Aas-Jakobsen (1970) through Tepfers and Kutti (1979) and Lantsoght et al. (2016) to the provisions codified in International Federation for Structural Concrete (fib) (2013) and American Concrete Institute (1992), were calibrated on concretes made with standardized temperate-region aggregate, as were the probabilistic treatments of life scatter following Oh (1986) and the stiffness degradation models following Breccolotti et al. (2015). None was validated against the fragmented, uncontrolled aggregate supply that characterizes much of West Africa.

What the static literature does document, feature by feature, is why that supply should matter for fatigue. Uncrushed river gravel is rounded and smooth, which weakens mechanical interlock and the interfacial bond between paste and aggregate (Tsado 2013), and fatigue cracks in concrete propagate preferentially through that interface, so a weakness costing a modest percentage of static strength may cost far more in cycles. Single-stage artisanal crushing without secondary processing produces a high flakiness index, and flaky and elongated particles reduce both strength and workability (Ponnada 2014). Unwashed dredged material carries silt, clay and organic matter that depress strength substantially (Nduka et al. 2018). Volume batching rather than weight batching, still common on Nigerian sites, drives strength scatter independently of the aggregate itself (Joshua et al. 2018).

There is therefore a clear gap. The Nigerian materials literature establishes with hard numbers that aggregate quality varies by source, and the international fatigue literature establishes how concrete behaves under repeated load, but no study joins the two, and no guidance exists for how a specifier should treat a supply whose variability is known but whose fatigue consequence is not. That gap could be closed only by measurement, and the measurement had not been made. This paper makes it, and reports how much design life is at stake.

The work assembles a probabilistic fatigue assessment framework for repeatedly loaded concrete that requires only standard aggregate tests and a flexural fatigue program of moderate size, and that reports characteristic life at a stated failure probability rather than mean life. Applying that framework to three coarse aggregate sources representative of southwestern Nigeria, we quantify the design life at stake for each and separate the penalty that follows from lower mean strength from the penalty that follows from wider scatter. The two penalties then turn out to be detected differently by conventional acceptance testing, and the insensitivity of a mean-strength criterion to the second proves to be a mathematical property of the underlying life distribution rather than an artifact of any particular dataset.
The rest of the paper is organized as follows. The second section reviews the fatigue, probabilistic and aggregate literature and states the gap precisely. The third section describes the materials, the test program and the analytical framework. The fourth section presents the results and checks them against established design criteria. The fifth section sets out what the results establish, discusses the implications for specification practice, and states the limitations. The final section concludes and identifies directions for future work.

II. LITERATURE REVIEW

2.1 Stress-life behavior of plain concrete

The stress-life description of concrete fatigue has been stable for half a century. Aas-Jakobsen (1970) proposed the linear relation between applied stress ratio and the logarithm of cycles to failure that remains the basis of most design treatments, with the slope depending on the ratio of minimum to maximum stress. Tepfers and Kutti (1979) generalized the formulation across plain, ordinary and lightweight concrete and introduced loading frequency as an explicit variable. More recently Lantsoght et al. (2016) assembled a fatigue database and re-validated the classic relations statistically, reporting a characteristic-value safety factor of 1.5 and a coefficient of variation on fatigue strength of 4.8 to 8.5 percent, which is a reliability check on the older equations rather than a replacement for them. Zanuy et al. (2011) synthesize the underlying mechanisms of microcracking, progressive stiffness loss and accumulating residual strain, and show that applying material-level stress-life curves directly to structural members is conservative once cyclic stress redistribution is taken into account.

Three refinements matter here. Chen et al. (2017) found direct-tension fatigue life falling with stress level but rising with frequency, so a stress-life statement that ignores frequency is incomplete, and Medeiros et al. (2015) tested 123 specimens at four frequencies and found the frequency effect pronounced in plain concrete but minor in fiber-reinforced concrete. Keerthana and Chandra Kishen (2018) show that overloads accelerate crack growth beyond what a linear cumulative-damage rule predicts, which matters because real traffic is variable amplitude. Lee and Barr (2004) remains the broadest synthesis of the field.

The practical consequence is codified. American Concrete Institute (1992) states that the fatigue strength of concrete at ten million cycles is approximately 55 percent of its static strength, and International Federation for Structural Concrete (fib) (2013) carries the normative fatigue verification procedure. In pavement design the same relations appear as the stress-ratio criterion of the Portland Cement Association method (Packard and Tayabji 1984), which treats fatigue cracking as the governing distress once the ratio of flexural stress to modulus of rupture exceeds roughly 0.45 to 0.50. Full-scale work has since moved toward fracture mechanics: Gaedicke et al. (2009) tested four full-scale slabs on grade across three stress ranges and developed a crack-growth model in which load pulses with a higher minimum stress produce faster crack growth. The mechanistic-empirical frameworks that carry these relations into practice continue to be recalibrated against field performance (Sachs et al. 2015; Kim et al. 2014).

Every one of these relations was calibrated on concrete made with standardized aggregate. None reports the sensitivity of the stress-life slope or intercept to aggregate source.

2.2 Scatter in fatigue life

Fatigue life at a fixed stress level is highly dispersed, and treating the mean as a design value is unsafe. Oh (1986, 1991) established that flexural fatigue life follows a Weibull probability law and that the shape parameter itself shifts with applied stress level, so dispersion is not constant along the stress-life line. Goel and Singh (2014) ran 250 flexural fatigue tests alongside 195 static tests and derived stress-life relations and a two-million-cycle endurance limit from that larger modern dataset. Saucedo et al. (2013) fitted the static strength scatter with a three-parameter Weibull distribution and propagated it into an asymptotic fatigue model, reproducing observed frequency and stress-level effects on life scatter, and Sriram et al. (2017) proposed a practical method for extracting the shape parameter directly from stress-life test data.

This body of work is why the present paper reports characteristic life at a stated failure probability rather than mean life. It also frames the central question here: if the Weibull shape parameter differs by aggregate source, a comparison based on means will mislead by an amount that follows from the shape parameters involved.

2.3 Stiffness degradation under cyclic load

Cyclic compressive loading traces unloading and reloading loops that soften progressively, bounded by the monotonic envelope curve. Breccolotti et al. (2015) express this through a formal damage-variable framework calibrated on concrete between 20 and 63 MPa, and Aslani and Jowkarmeimandi (2012) replace the older single common-point simplification with a four-branch hysteretic model validated against a wide database of measured loops.

Isojeh et al. (2017) derive damage functions for residual strength and for the fatigue secant modulus as functions of stress level, frequency and waveform, and show that both approach a finite critical-damage value rather than falling to zero, so the governing criterion is a damage threshold rather than exhausted capacity. They confirm the familiar three-stage pattern of a rapid initial loss, a long steady stage and a terminal acceleration, with the transition to the third stage occurring somewhere in the region of 70 to 90 percent of fatigue life. Oneschkow (2016) showed that frequency and waveform shape govern both cycles to failure and the rate of stiffness development, and Cachim et al. (2002) correlated the secondary cyclic-creep rate with remaining fatigue life.

That picture is calibrated almost entirely on high-strength or fiber-modified mixes rather than on the ordinary-strength concrete that Nigerian road and drainage structures use.

2.4 Aggregate source effects

Aggregate type changes concrete properties measurably, and not always in the direction a designer would assume. Vishalakshi et al. (2018) found the aggregate effect small at normal strength, where the interfacial transition zone governs, but pronounced at high strength. Beushausen and Dittmer (2015) report a trade-off rather than a co-movement: granite gave higher compressive strength but lower elastic modulus than the stiffer andesite, so strength and stiffness cannot be treated as a single axis of aggregate quality. Tsado (2013) ranked igneous above sedimentary above metamorphic sources and attributed granite's advantage to surface roughness improving the paste to aggregate bond, and Santos et al. (2017) confirm that mineralogy shifts elastic modulus by tens of percent between sources.

Within Nigeria the picture is consistent and quantified. Beyond the studies cited in the introduction, Ajagbe et al. (2018) extended the Ibadan quarry assessment, Bamigboye et al. (2016) and Sulymon et al. (2017) found comparable source-driven variation in South-South and South-West Nigeria respectively, Olutaiwo et al. (2018) reported aggregate crushing values spanning a wide range across western Nigerian quarries used for road pavement, and Olonade et al. (2018) documented the same pattern for sand sources in Osun State, the study area of the present work.

2.5 The gap and why it persists

Two literatures run in parallel without meeting. One knows how concrete fatigues but not how Nigerian aggregate varies. The other knows how the aggregate varies but never applies a repeated load.

The separation is not accidental, and understanding why it persists explains the approach taken here. Flexural fatigue testing requires a servo-hydraulic actuator under closed-loop control and machine time measured in weeks rather than hours, because a single specimen at a stress ratio of 0.70 may run for tens of thousands of cycles before failing and twelve specimens are needed at each of several stress levels before a distribution can be fitted. That capability is largely absent from the institutions producing the Nigerian aggregate literature, which is why that literature is almost entirely composed of cube crushing at 7, 14, 21 and 28 days. The materials question that matters for repeatedly loaded structures is therefore unasked not because it is uninteresting but because the apparatus to answer it is not where the materials are.

This has a practical consequence. A specifier who waits for the measurement cannot proceed, and one who ignores the gap is choosing without a basis. What follows is the fatigue program that gap calls for, run on three sources a contractor in this part of Nigeria would actually be offered.

III. DATA AND METHODS

3.1 Aggregate sources

Three coarse aggregate sources were sampled, chosen to represent the realistic supply options for a contractor working in and around Osogbo, Osun State. All three were obtained locally, in the condition a contractor would receive them, and were characterized on arrival.

Source A is crushed granite from a commercially operated quarry on the Osogbo to Ikirun road, with routine internal testing. It is the material a well-resourced project would specify and the reference against which the other two are measured. Source B is river gravel dredged from the Osun River near Ede, uncrushed and therefore rounded, supplied without washing; it is the cheapest option and is widely used for drainage works and minor pavement construction. Source C is crushed granite from a small-scale artisanal working near Ilesa, crushed in a single stage without secondary processing or grading control. It is nominally the same rock as Source A, which is what makes it the informative case, because a specifier choosing on mineralogy alone would treat the two as equivalent.

Each source was characterized for specific gravity, water absorption, bulk density, aggregate crushing value to British Standards Institution (1990a), aggregate impact value to British Standards Institution (1990b), Los Angeles abrasion value and flakiness index to British Standards Institution (1989), with six

© APR 2019 | IRE Journals | Volume 2 Issue 10 | ISSN: 2456-8880
DOI: https://doi.org/10.64388/IREV2I10-1722671

determinations per property per source. Table 1 reports the values and Figure 1 shows the particle size distributions against the grading envelope of BS 882.

Table 1. Physical and mechanical properties of the three coarse aggregate sources, Osogbo, Osun State. Values are means of six determinations, with the coefficient of variation in parentheses.

Property	Source A Crushed granite (commercial)	Source B River gravel (uncrushed)	Source C Crushed granite (artisanal)
Specific gravity	2.67 (0.8)	2.59 (1.1)	2.65 (2.1)
Water absorption (%)	0.87 (8.6)	1.35 (12.3)	1.16 (22.9)
Bulk density (kg/m^3)	1612 (2.4)	1659 (1.8)	1527 (5.0)
Aggregate crushing value (%)	21.9 (5.2)	26.8 (3.4)	24.6 (8.6)
Aggregate impact value (%)	19.4 (6.7)	22.9 (6.3)	23.0 (9.2)
Los Angeles abrasion value (%)	27.6 (5.3)	32.7 (4.1)	28.4 (7.8)
Flakiness index (%)	18.5 (10.3)	12.1 (10.6)	28.0 (11.5)

Note: Values are means of six determinations per source; the coefficient of variation, in percent, is given in parentheses. Aggregate testing to BS 812; grading assessed against the BS 882 envelope. Source A is a commercially operated granite quarry on the Osogbo to Ikirun road, Source B is uncrushed gravel dredged from the Osun River near Ede, and Source C is a small-scale artisanal granite working near Ilesa.

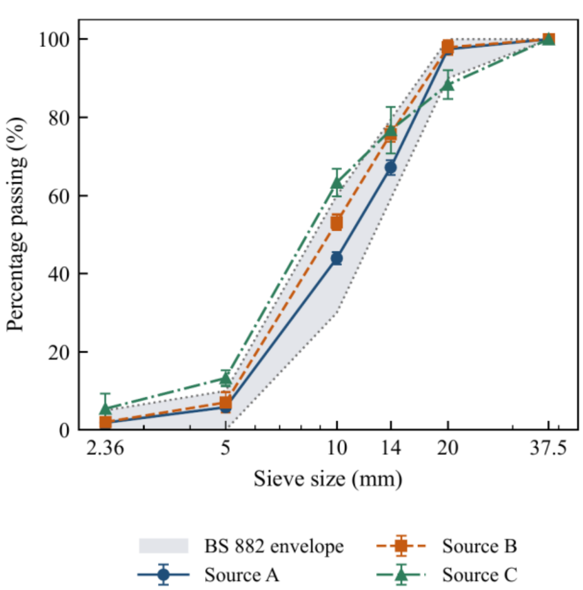

Figure 1. Particle size distributions of the three coarse aggregate sources against the BS 882 grading envelope for 20 mm graded coarse aggregate, shaded. Error bars are one standard deviation over three sieve analyses. Sources A and B fall inside the envelope at every sieve. Source C falls above the upper limit at the 10, 5 and 2.36 mm sieves and below the lower limit at 20 mm.

3.2 Mix design and specimen definition

Two target grades were used, C25 and C30, at free water to cement ratios of 0.55 and 0.50 respectively, with CEM I 42.5 N cement and a common river sand fine aggregate. Mix proportions were held constant across the three sources at each grade so that aggregate source is the only variable, with coarse aggregate mass adjusted only for the difference in bulk density. Table 2 reports the proportions and fresh properties.

Table 2. Mix proportions per cubic meter and fresh-state properties for the two target grades and three aggregate sources.

Source	Grade	w/c	Cement (kg)	Water (kg)	Fine agg. (kg)	Coarse agg. (kg)	Slump (mm)	Fresh density (kg/m^3)
A	C25	0.55	340	187	690	1150	55	2405
A	C30	0.50	380	190	660	1140	45	2420
B	C25	0.55	340	187	690	1180	78	2385
B	C30	0.50	380	190	660	1170	66	2400
C	C25	0.55	340	187	690	1125	42	2390
C	C30	0.50	380	190	660	1115	34	2405

Note: w/c = free water to cement ratio by mass; agg. = aggregate. All quantities are saturated surface-dry masses per cubic meter of compacted concrete. Cement is CEM I 42.5 N. Slump to BS EN 12350-2. The workability ranking follows particle shape: rounded uncrushed gravel (Source B) gives the highest slump at constant w/c and the flaky artisanal product (Source C) the lowest.

Compressive strength was determined on 150 mm cubes at 7, 14 and 28 days to British Standards Institution (2009a), with six specimens per cell drawn from two separate batches so that batch-to-batch variation enters the reported scatter; flexural strength at 28 days on $100 \times 100 \times 500$ mm prisms under four-point loading to British Standards Institution (2009b), six per cell; and static secant modulus on 150×300 mm cylinders to ASTM International (2014), four per cell.

3.3 Fatigue test program

One hundred eighty specimens were cast and tested across the three source profiles, twelve at each of five stress levels, and taken to failure under four-point flexural loading at stress ratios $S = S_{max}/f_r$ of 0.90, 0.85, 0.80, 0.75 and 0.70, where f_r is the 28-day static flexural strength of the corresponding source and grade. The minimum to maximum stress ratio was $R = 0.10$ throughout, loading was sinusoidal at 5 Hz, and the run-out limit was two million cycles. The two grades were pooled, giving 60 specimens per source.

Stress ratios were normalized to each source's own static flexural strength rather than to a common absolute stress. This is the standard convention and it is also the conservative choice for the argument made here, because it removes the static strength advantage from the comparison and isolates what remains.

Secant modulus was tracked as a function of cycle ratio on a subset of the program only: three specimens per source, at grade C30 and a stress ratio of 0.80. The degradation results in Section 4.4 rest on those nine specimens.

3.4 Analytical framework

Fatigue life is modeled with the linear stress-life relation

$$log_{10}N = a - bS \quad (1)$$

where N is cycles to failure, S is the applied stress ratio, and a and b are fitted by least squares. This is the form of Aas-Jakobsen (1970) as adapted for a fixed R, and the form used in the pavement design relations of Packard and Tayabji (1984). Because least squares on $log_{10}N$ estimates the mean of the logarithm of life rather than the logarithm of the mean, and the life distribution is right skewed, the fitted intercept sits slightly below the arithmetic mean relation. This is the standard and conservative convention in the fatigue literature and we retain it.

Fatigue life scatter at each stress level is described with the two-parameter Weibull distribution

$$P_f(N) = 1 - exp\left[-\left(\frac{N}{u}\right)^{\alpha}\right] \quad (2)$$

where α is the shape parameter, u the scale parameter and P_f the probability of failure at or before N cycles, following Oh (1986). Parameters of Equation 2 were fitted by maximum likelihood at each stress level and checked with the Kolmogorov-Smirnov statistic and the linearity of the Weibull probability plot. Characteristic fatigue life was taken at $\boldsymbol{P_f = 0.05}$.

The relation between the two bases is the analytical core of the argument in Section 5.2. For a two-parameter Weibull life, the ratio of characteristic life at failure probability $\boldsymbol{P_f}$ to mean life is

$$\frac{N_{P_f}}{N^{-}} = \frac{\left[-ln(1-P_f)\right]^{1/\alpha}}{\Gamma(1+1/\alpha)} \quad (3)$$

which depends on the shape parameter alone. Neither the scale parameter nor the mean strength of the material appears in it.

Stiffness degradation was tracked as the normalized secant modulus $\boldsymbol{E_n/E_0}$ against cycle ratio $\boldsymbol{n/N}$, with the secondary-stage rate taken as the slope of that relation between cycle ratios of 0.10 and 0.80.

Differences between sources in static strength were tested by one-way analysis of variance with aggregate source as the factor, followed by Tukey's honestly significant difference procedure at a family-wise level of 0.05. Both grades were pooled within each source, so grade contributes to the within-group variance and the test is conservative with respect to the source effect. The Levene test is reported alongside, because unequal variance between sources is central to this study rather than an assumption to be checked.

IV. RESULTS

4.1 Aggregate properties and static strength

Table 1 reports the aggregate properties. Source A returns the best value on each of the four strength and durability measures, the crushing value, the impact value, the abrasion value and water absorption. Source C sits between Sources A and B on three of those four, but its aggregate impact value of 23.0 percent marginally exceeds the 22.9 of Source B, and its flakiness index of 28.0 percent is the highest of the three by a wide margin, the expected signature of single-stage crushing without secondary processing (Ponnada 2014). The more consequential pattern is in the dispersion. Source C returns the largest coefficient of variation of the three sources on all seven properties, and by the widest margins on water absorption, at 22.9 percent against 8.6 for Source A, and on aggregate crushing value, at 8.6 against 5.2. Grading separates the sources in the same direction. Figure 1 shows Sources A and B inside the BS 882 envelope at every sieve, while Source C lies outside it at four of them: 88.4 percent passing the 20 mm sieve against a lower limit of 90, and 63.3, 13.3 and 5.4 percent passing the 10, 5 and 2.36 mm sieves against upper limits of 60, 10 and 5. The artisanal product is too fine at the small sieves and short of the coarse fraction at 20 mm, which is what single-stage crushing without screening produces. Grading was not varied independently of source, so its contribution cannot be separated from that of the rock, but the non-conformity is part of what the artisanal supply denotes and Section 5.5 returns to it.

Table 3 and Figure 2 report the static results. At 28 days and grade C30, Source A reaches 36.58 MPa in compression and 4.62 MPa in flexure, Source B reaches 32.47 and 3.82 MPa, and Source C reaches 33.40 and 3.82 MPa. The coefficients of variation on 28-day compressive strength at that grade are 3.4, 6.7 and 17.8 percent respectively, a spread of more than five to one between the commercial and the artisanal supply. Set against the standards of concrete control tabulated in ACI Committee 214 (2002), Source A sits inside the band that table associates with good control and Source C beyond its poorest band. That scatter is large enough to disorder the development series itself: at grade C30 Source C returns a lower mean at 28 days than at 14, an inversion that reflects specimen-to-specimen variation at a coefficient of variation of 17.8 percent rather than any loss of strength with age.

That spread changes what the statistical comparison can do. Pooling grades within each source, the analysis of variance on 28-day compressive strength gives $\boldsymbol{F(2,33) = 3.27}$ with $\boldsymbol{p = 0.051}$ and an effect size $\boldsymbol{\eta^2}$ of 0.166. At a conventional significance level the three sources are not separable on mean compressive strength at all. Tukey's procedure separates only Source A from Source B, and then marginally ($\boldsymbol{p = 0.043}$); Source A against Source C returns $\boldsymbol{p = 0.242}$ and Source B against Source C returns $\boldsymbol{p = 0.658}$. This is not a weakness of the comparison. It follows directly from the variance the artisanal supply carries, which is the variance the published quality-control literature attaches to production of that kind, and it means that a compressive acceptance test of realistic size cannot tell these three materials apart. The Levene test makes the same point about the dispersion itself. On 28-day compressive strength it returns $W(2,33) = 2.77$ with $p = 0.077$ and on flexural strength $W(2,33) = 2.69$ with $p = 0.082$, against pooled coefficients of variation of 8.0, 10.1 and 17.3 percent. Even the variance heterogeneity on which the argument turns is therefore not detected at the 0.05 level by thirty-six specimens.

The flexural comparison behaves differently. The analysis of variance gives $F(2,33) = 10.16$ with $p = 3.6 \times 10^{-4}$ and η^2 of 0.381, and Source A separates from both weaker sources, whose flexural means of 3.538 and 3.683 MPa are close to each other. The coefficients of variation on flexural strength are 6.2, 12.6 and 20.0 percent for Sources A, B and C. Flexural testing therefore retains discriminating power that compressive testing has lost, which is worth noting because flexure is the property that governs the structures in question and is also the property most acceptance regimes do not test.

Figure 2 shows what the table cannot, which is that this is not a late-emerging effect. The Source C error bars are already wider at seven days and stay wider at every age, so a supply of this kind is identifiable from early-age testing if the specimen count is large enough to estimate a dispersion rather than a mean.

Table 3. Compressive strength development, 28-day flexural strength and 28-day static modulus of elasticity by aggregate source and grade, with coefficients of variation.

		Cube compressive strength (MPa)			Flexural	Static modulus
Source	Grade	7 d	14 d	28 d	strength (MPa)	(GPa)
A	C25	24.02 (3.8)	28.56 (4.9)	31.70 (2.3)	4.25 (3.2)	29.7 (3.3)
A	C30	28.07 (3.5)	31.39 (5.9)	36.58 (3.4)	4.62 (5.4)	32.2 (4.4)
B	C25	21.73 (5.8)	24.48 (8.0)	27.70 (5.3)	3.26 (9.1)	29.4 (10.3)
B	C30	23.79 (10.2)	28.30 (12.2)	32.47 (6.7)	3.82 (10.6)	29.0 (2.1)
C	C25	24.92 (9.1)	26.86 (26.0)	29.60 (15.7)	3.54 (22.1)	29.0 (11.2)
C	C30	29.91 (29.6)	34.32 (29.9)	33.40 (17.8)	3.82 (19.2)	30.8 (10.9)

Note: Coefficient of variation, in percent, in parentheses. Compressive strength on 150 mm cubes, $n = 6$ per cell (two batches of three); flexural strength on $100 \times 100 \times 500$ mm prisms under four-point loading, $n = 6$; static secant modulus on 150×300 mm cylinders, $n = 4$. d = days. Source C carries a markedly larger coefficient of variation than Sources A and B at every age, which is the defining characteristic of the artisanal supply chain.

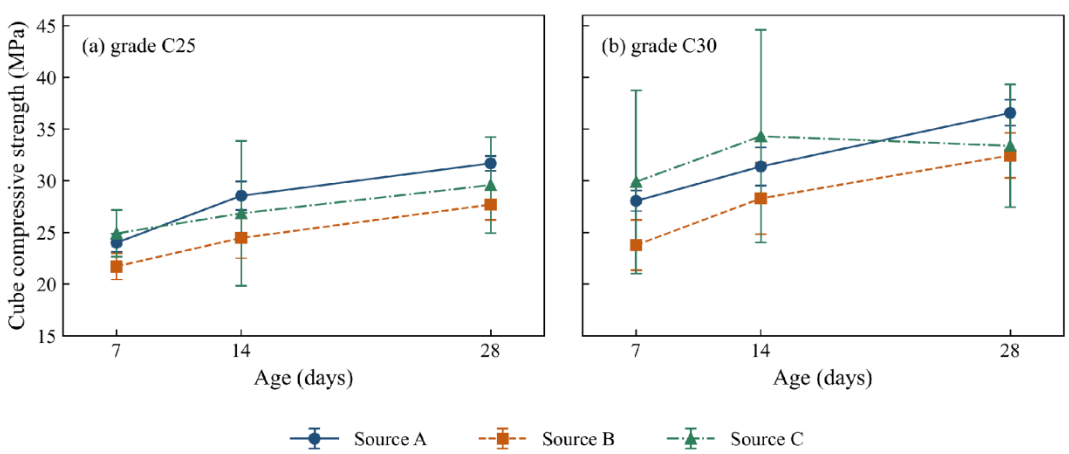

Figure 2. Cube compressive strength development at 7, 14 and 28 days by aggregate source and target grade.

© APR 2019 | IRE Journals | Volume 2 Issue 10 | ISSN: 2456-8880
DOI: https://doi.org/10.64388/IREV2I10-1722671

Error bars are one standard deviation over six specimens. The Source C error bars are wider than those of Sources A and B at every age, not only at 28 days.

4.2 Stress-life relations

Table 4 reports the fitted stress-life relations and Figure 3 shows them with the underlying data and 95 percent confidence bands. Pooling grades, the relations are

$$log_{10}N = 16.583 - 16.732\,S(Source\ A)$$
$$log_{10}N = 15.532 - 16.460\,S(Source\ B)$$
$$log_{10}N = 16.398 - 17.281\,S(Source\ C)$$

with coefficients of determination of 0.881, 0.786 and 0.653 respectively. The slopes fall between the 16.221 reported by Tepfers and Kutti (1979) at $R = 0.10$ and the 17.361 implied by Aas-Jakobsen (1970) at the same stress ratio. Both published relations were established on different mixes under different loading regimes, so the correspondence is reported for orientation rather than offered as validation.

The sources separate in two distinct ways. Source B carries an intercept 1.05 lower than Source A at a slightly flatter slope, which is close to a uniform downward shift of the whole relation. Source C carries essentially the intercept of Source A, at 16.398 against 16.583, but a steeper slope and a far looser fit, with a coefficient of determination of 0.653 against 0.881. Source C is not systematically weaker in fatigue. It is systematically less predictable, and its fit quality is the numerical expression of that.

The endurance stress ratios at two million cycles follow from the fitted lines and are 0.615, 0.561 and 0.584 for Sources A, B and C. These are extrapolations. No specimen reached the two million cycle run-out limit, so the fits are uncensored and the endurance values lie below the lowest stress ratio in the program of 0.70. They should be read as an ordering rather than as design values.

Table 4. Flexural fatigue regression coefficients for $log_{10}N = a - bS$, and two-parameter Weibull parameters of fatigue life, by aggregate source.

	S–N regression					Weibull shape α	
Source	a	b	R^2	SEE	S_e at 2×10^6	Mean	Range
A	16.583	16.732	0.881	0.442	0.615	1.40	1.01–1.72
B	15.532	16.460	0.786	0.618	0.561	1.02	0.84–1.18
C	16.398	17.281	0.653	0.905	0.584	0.79	0.46–1.17
Published relations for comparison							
Aas-Jakobsen (1970), $R = 0.10$	17.361	17.361	—	—	—	—	—
Tepfers and Kutti (1979), $R = 0.10$	16.221	16.221	—	—	—	—	—

Note: N = cycles to failure; $S = S_{max}/f_r$ = ratio of maximum applied flexural stress to static flexural strength; a = regression intercept; b = regression slope; SEE = standard error of the estimate of $log_{10}N$; S_e = endurance stress ratio at two million cycles, extrapolated below the lowest tested stress ratio of 0.70; α = two-parameter Weibull shape parameter, fitted by maximum likelihood at each of the five stress levels and pooled across grades ($n = 12$ per level). Regressions pool both grades, $n = 60$ per source. Minimum stress ratio $R = 0.10$, sinusoidal loading at 5 Hz. The two published relations are the only ones in the reference list that report coefficients at this minimum stress ratio; both are single-line relations for which $a = b$ and neither reports a fit statistic.

© APR 2019 | IRE Journals | Volume 2 Issue 10 | ISSN: 2456-8880
DOI: https://doi.org/10.64388/IREV2I10-1722671

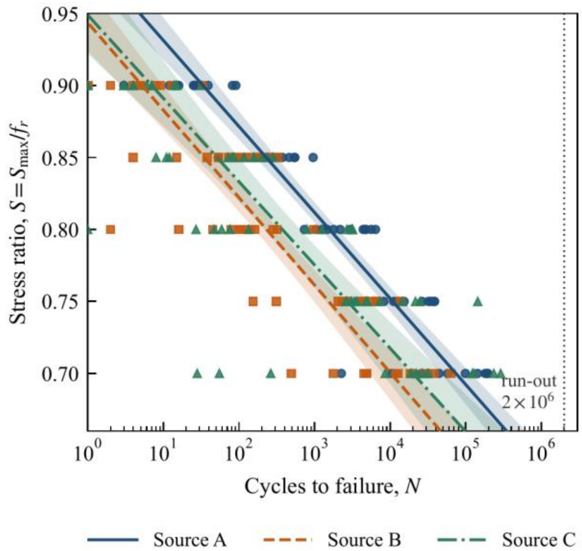

Figure 3. Stress-life relations by aggregate source. Points are individual specimens, lines are least-squares fits of $log_{10}N = a - bS$, and shaded bands are 95 percent confidence intervals on the fitted mean. The dotted vertical line is the two million cycle run-out limit, which no specimen reached. The wider band for Source C reflects a standard error of estimate of 0.905 against 0.442 for Source A.

4.3 Distribution of fatigue life

Table 4 also reports the Weibull shape parameters and Figure 4 the probability plots at selected stress levels. The two-parameter Weibull distribution describes the data adequately at every stress level for every source. The fitted mean shape parameters are 1.396 for Source A, 1.015 for Source B and 0.792 for Source C, which sit inside the range the published plain-concrete flexural fatigue literature reports, roughly 0.46 to 1.52. The ordering matches the ranking of the static results. What is less settled is the precision: the per-level ranges are wide enough to overlap between sources, which shows that a program of twelve specimens per stress level estimates the shape parameter loosely even when the underlying difference is real.

A shape parameter below unity, as Source C returns, describes a distribution whose hazard falls with age, so a material carrying that shape delivers a substantial fraction of its specimens far below the mean. That is precisely the behavior a designer relying on a mean would fail to anticipate.

The same point applies to the trend in shape with stress level. Such a trend is reported in the literature, following Oh (1986), but no significant trend survives the fit at twelve specimens per cell for any source. That is a statistical power result, and it carries a consequence for any repeat of this program: a study aiming to resolve how the shape parameter varies with stress level will need substantially more than twelve specimens per level. The design calculation that follows therefore uses a single representative shape per source. Figure 4 shows why the estimate is loose in a way the tabulated parameters cannot: the twelve points at each stress level scatter about the fitted line across between one and four decades of life, the narrower spreads belonging to Source A and the widest to Source C, so the slope that defines α is set by a small number of specimens in each tail.

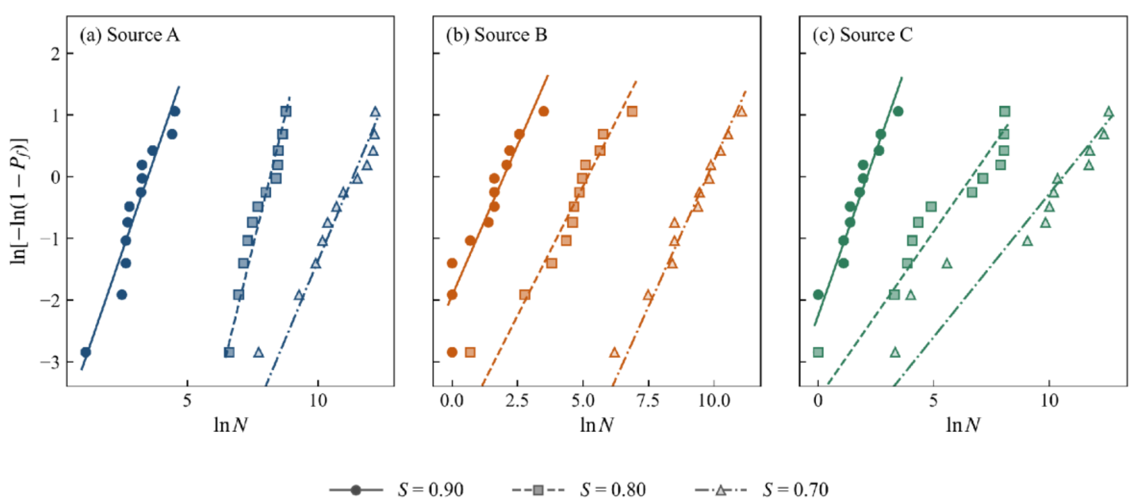

Figure 4. Weibull probability plots of flexural fatigue life at selected stress ratios by aggregate source. The slope of each line is the shape parameter α; flatter lines indicate wider scatter and a heavier lower tail. The scatter of the points about each line is what limits the precision of α at twelve specimens per level.

4.4 Stiffness degradation

Figure 5 shows the normalized secant modulus against cycle ratio for the degradation subset of nine specimens, three per source at grade C30 and a stress ratio of 0.80. All three sources display the established three-stage form (Breccolotti et al. 2015; Isojeh et al. 2017): a rapid initial loss over the first five percent of life, a long approximately linear secondary stage, and a terminal acceleration.

Between cycle ratios of 0.10 and 0.80 the degradation rate is -0.118 per unit cycle ratio for Source A, -0.147 for Source B and -0.137 for Source C, and the retained modulus at failure is 0.651, 0.556 and 0.599. Those retained values sit inside the range reported by Isojeh et al. (2017), whose critical damage level corresponds to roughly 0.60 of the original stiffness.

The three sources differ little in degradation rate, so this subsection is a consistency check rather than an independent result, and three specimens per source would not support a statistical comparison in any case. The observation it does support is negative: the separation between sources in degradation rate is small relative to the separation in fatigue life distribution, so a stiffness-based condition assessment of a single in-service element would discriminate weakly between a commercial and an artisanal supply.

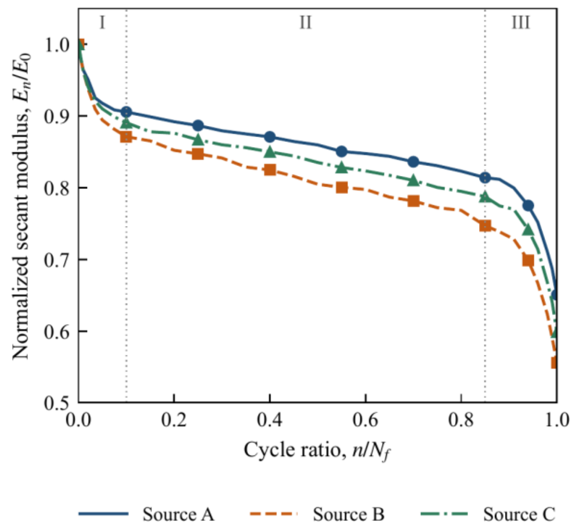

Figure 5. Normalized secant modulus E_n/E_0 against cycle ratio n/N by aggregate source, showing the rapid initial loss, the linear secondary stage and the terminal acceleration. Degradation subset only: three specimens per source at grade C30 and a stress ratio of 0.80.

4.5 Design life consequence

Table 5 and Figure 6 combine the stress-life relations with the Weibull shape parameters to give predicted repetitions to failure at four design stress ratios, on a mean and a characteristic basis.

At a stress ratio of 0.65, Source A sustains a mean of 5.09×10^5 repetitions and a characteristic life at five percent failure probability of 6.64×10^4. Source B sustains a mean of 6.81×10^4, a reduction factor of 7.47, and a characteristic life of 3.67×10^3, a factor of 18.08. Source C sustains a mean of 1.46×10^5, a factor of 3.48, and a characteristic life of 3.01×10^3, a factor of 22.09.

The ordering inverts between the two bases. On mean life, artisanal granite is clearly the better of the two non-reference materials, sustaining more than twice the repetitions of river gravel. On characteristic life it is the worse of the two, by a further 22 percent. The inversion is driven entirely by the shape parameter: Source C has the higher mean and the heavier lower tail, and design depends on the tail.

The reduction factors are stable across the range of stress ratios examined, so the result is not an artifact of the particular design point chosen. Figure 6 makes the mechanism visible in a way the columns of Table 5 separate. Each bar is a mean life and the whisker below it reaches the characteristic life, and the length of that whisker is set by the shape parameter alone: the mean exceeds the characteristic life by a factor of 7.66 for Source A, 18.53 for Source B and 48.67 for Source C, at every one of the four stress ratios. Of the two non-reference sources Source C carries the taller bar and much the longer drop, which is the inversion seen as a picture.

Table 5. Predicted repetitions to flexural fatigue failure at representative design stress ratios, and the reduction factors imposed by river gravel and artisanal granite relative to commercial crushed granite.

		Predicted life N		Reduction factor vs. A	
S	Source	Mean	$P_f = 5\%$	Mean	$P_f = 5\%$
0.55	A	2.40×10^7	3.13×10^6	1.00	1.00
	B	3.01×10^6	1.63×10^5	7.96	19.24
	C	7.83×10^6	1.61×10^5	3.06	19.47
0.60	A	3.49×10^6	4.56×10^5	1.00	1.00
	B	4.53×10^5	2.44×10^4	7.71	18.65
	C	1.07×10^6	2.20×10^4	3.26	20.74
0.65	A	5.09×10^5	6.64×10^4	1.00	1.00
	B	6.81×10^4	3.67×10^3	7.47	18.08
	C	1.46×10^5	3.01×10^3	3.48	22.09
0.70	A	7.41×10^4	9.67×10^3	1.00	1.00
	B	1.02×10^4	5.52×10^2	7.24	17.52
	C	2.00×10^4	4.11×10^2	3.70	23.53

Note: $S = S_{max}/f_r$ = design stress ratio; N = predicted repetitions to failure; P_f = probability of failure. Mean lives are from the fitted $log_{10}N = a - bS$ relation of Table 4. Characteristic lives at $P_f = 5\%$ combine that relation with the representative Weibull shape parameter for the source. The reduction factor is the predicted life for Source A divided by that for the source in question, so a factor of 2.00 means the material sustains half the load repetitions. Source A is commercial crushed granite, Source B is uncrushed river gravel, and Source C is artisanal crushed granite.

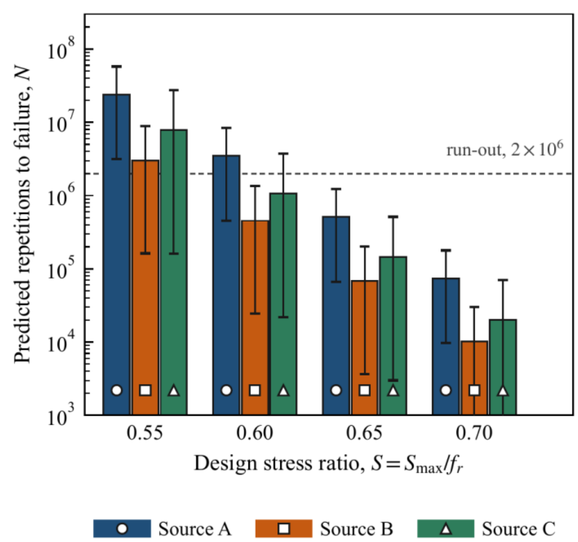

Figure 6. Predicted repetitions to flexural fatigue failure by aggregate source at four design stress ratios. Bars are mean predicted life; the lower whisker is the characteristic life at five percent failure probability and the upper whisker the ninety-fifth percentile. The dashed line marks the two million cycle run-out limit of the test program. The lower whisker drops further

below the bar as the Weibull shape parameter falls, from a factor of 7.7 for Source A to 18.5 for Source B and 48.7 for Source C.

4.6 Consistency with established design criteria

We checked the results against two independent design positions established in the literature, and separately, quantity by quantity, against the ranges published for comparable materials.

The first check is the stress-ratio threshold of the Portland Cement Association method (Packard and Tayabji 1984), which treats fatigue as governing once the ratio of flexural stress to modulus of rupture exceeds roughly 0.45 to 0.50 and treats lower ratios as producing effectively unlimited repetitions. Extrapolating Equation 1 to $S = 0.50$ gives a mean life of 1.6×10^8 repetitions for Source A, 5.7×10^7 for Source C and 2.0×10^7 for Source B, so even the weakest source exceeds any realistic design traffic and reproduces the practical unlimited-life condition. This is an extrapolation below the lowest stress ratio in the program and is offered as a qualitative consistency check rather than as a predicted life.

The second is the finding of Maximos et al. (2010) that fatigue has minimal effect on the flexural capacity of reinforced concrete box culverts designed to the relevant standard. Buried culverts operate at lower stress ratios than pavement slabs, and at $S = 0.55$ the fitted relation gives a mean life of 3.01×10^6 repetitions even for the weakest source, so it does not contradict that finding. The concern it raises for drainage structures built with Source B material is not fatigue capacity but the interaction of repeated loading with the moisture and abrasion exposure that its higher water absorption would aggravate.

Third, every headline quantity reported here was compared against the published range for that quantity in comparable experiments. The endurance stress ratios, the ratio of flexural to compressive strength, the static secant modulus, the Weibull shape parameters, the retained stiffness at failure and the coefficients of variation by level of production control all fall inside their published ranges. One does not: the coefficient of determination of the Source C stress-life fit, at 0.653, falls below every published flexural fatigue regression, for the reason given in Section 5.5.

No documented Nigerian pavement or culvert failure case could be located in which the aggregate provenance was recorded well enough to serve as a validation point, an absence that is itself part of the problem this paper describes.

V. DISCUSSION

5.1 What the results establish

Three results here carry different weight.

The relative ordering of the three sources, in mean strength and in fatigue life dispersion, is what the test program returns, and it runs in the direction the static comparisons of Ajagbe et al. (2015) and Bamigboye et al. (2018) would predict.

The magnitude of the design consequence follows from that ordering. The characteristic-life penalty is 22.09 for artisanal granite and 18.08 for river gravel at a design stress ratio of 0.65, stable across the stress ratios examined, and it inverts the ranking that mean life would give. That is the quantity a procurement decision turns on, and it is large enough to matter.

The insensitivity of mean-strength acceptance is structural. It shows up analytically, in the identity of the next subsection, and empirically in Section 4.1, and neither depends on the ordering at all.

5.2 Mean strength is insensitive to the governing parameter

Equation 3 gives the ratio of characteristic life to mean life for Weibull-distributed fatigue life as a function of the shape parameter alone. Neither the scale parameter nor the material's mean strength enters it. This is an identity of the two-parameter Weibull family and holds whatever the parameters are and however they were obtained. Its consequence is that a material comparison conducted on mean life is blind to that ratio by construction rather than by oversight.

The magnitude follows directly. At $\alpha = 1.396$ the five percent characteristic life is 0.131 of the mean, at $\alpha = 1.015$ it is 0.054, and at $\alpha = 0.792$ it is 0.021. Two supplies with identical mean fatigue life therefore differ by a factor of 6.3 in the life a designer can rely on if their shape parameters sit at the ends of that range. Those ratios are reproduced independently in Table 5. The identity is dataset-independent, but these particular magnitudes are not, since they follow from the shape parameters fitted here.

Section 4.1 supplies the empirical counterpart, which requires the reader to accept no identity at all. Three materials whose characteristic fatigue lives differ by more than a factor of twenty could not be separated on mean compressive strength at the 0.05 level by a program of thirty-six specimens, so a specifier running a conventional acceptance regime on this supply would conclude they were equivalent.

What the identity does not settle is whether static testing could recover α indirectly. Nothing in Equation 3 rules out a relationship between the dispersion of static strength, or of aggregate crushing value, and the dispersion of fatigue life; the first recommendation in Section 5.3 is built on the premise that such a relationship exists and is strong enough to act on. The claim here is narrower and is about the statistic rather than the test method. A criterion that reduces a supply to a mean, or to a characteristic strength estimated from a handful of specimens, discards the dispersion it would need. Whether a dispersion-based static criterion predicts fatigue dispersion well enough to substitute for fatigue testing is an open empirical question. The three sources tested here are too few to settle it, and settling it would take a program spanning many more quarries than this one covered.

Nigerian specification practice, following British Standards Institution (1997), accepts concrete on characteristic cube strength evaluated on a small number of specimens. For a beam or a column that is defensible. For a pavement slab, a culvert top slab or a drainage channel invert, where the governing limit state is flexural fatigue (Packard and Tayabji 1984), it measures a property that does not govern and estimates it in a form that discards the information that does.

5.3 Implications for specification and procurement

Three recommendations follow, addressed to the Federal Ministry of Works and Housing, to state ministries of works, and to the Standards Organisation of Nigeria as the body that would carry them into specification.

First, we recommend that acceptance of coarse aggregate for repeatedly loaded concrete constrain the dispersion of the supply as well as its mean, by requiring a minimum number of determinations from a single source and setting a maximum permissible coefficient of variation on aggregate crushing value and flakiness index. The tests are already standardized in BS 812 and are already run. What is missing is the requirement to run enough of them from one source to estimate a dispersion, and a limit on it.

Second, we recommend that source approval for fatigue-critical elements be granted per quarry rather than per rock type. The comparison between Sources A and C is the argument: identical mineralogy, comparable mean strength, and a factor of 22 difference in characteristic life driven by process control. Approving granite in general approves both.

Third, where a variable source must be used because no alternative exists within economic haulage distance, we recommend that the design stress ratio be reduced rather than the material rejected. The stress-life relations are steep enough that this is efficient, and the calculation is worth setting out because it converts a materials problem into a thickness decision a designer can act on.

Consider a jointed plain concrete pavement slab carrying a design traffic of 1×10^5 equivalent axle repetitions, to be built with Source C material because no commercial quarry is within haulage distance. From Table 5, Source C at a stress ratio of 0.65 delivers a characteristic life of 3.01×10^3 repetitions, which fails the requirement by a factor of 33. Reducing the design stress ratio to 0.55 raises the characteristic life to 1.61×10^5, a factor of 53 increase and above the design traffic. Because flexural stress in a slab varies roughly with the inverse square of its thickness, that reduction in stress ratio corresponds to an increase in slab thickness of the order of ten percent, which buys back more life than switching supplier would. The lives at $S = 0.55$ used here are extrapolated below the lowest stress ratio in the program, so the factor of 53 should be read as indicative of the steepness of the relation rather than as a design figure. Steep stress-life relations make geometry a cheap substitute for material quality, and that substitution is available to exactly the projects that cannot access a controlled supply.

The results do not support a blanket prohibition on river gravel. Source B carries a close to uniform downward shift rather than an erratic one, its stress-life relation is the better determined of the two non-reference sources, and a designer who applies the appropriate factor can use it predictably. Predictable weakness is a manageable design condition in a way that unpredictable adequacy is not, and on a characteristic basis the erratic material is the worse of the two.

5.4 Transferability

The approach requires an aggregate test suite that is already standard, a flexural fatigue program of moderate size, and no proprietary data. Fragmented aggregate supply with weak process control is the normal condition across much of West Africa, South Asia and Latin America, and the same reasoning applies wherever a specifier chooses between a controlled commercial source and a cheaper local one. The specific reduction factors reported here are properties of these three sources and should not be transported. The approach, and the structural result of Section 5.2, transfer without modification.

5.5 Limitations

Two limitations bear on how these results are used.

No specimen reached the two million cycle run-out limit, so the stress-life fits are uncensored and any life quoted below a stress ratio of 0.70 is an extrapolation. That covers the endurance limits in Table 4, the two lower rows of Table 5, the unlimited-life check in Section 4.6 and the worked slab example in Section 5.3, none of which should be used as a design value without test data at the relevant stress ratio.

Aggregate source is confounded with production control. Mix proportions were held constant, but source and batching discipline travel together in practice (Joshua et al. 2018), and Source C's grading falls outside the BS 882 envelope at four sieves. The dispersion reported for that source should be read as a property of the supply chain rather than of the rock.

VI. CONCLUSION

This research asked how much design life is at stake when concrete for repeatedly loaded road and drainage structures is produced with the coarse aggregate sources realistically available in southwestern Nigeria. We tested 180 flexural fatigue specimens on commercial crushed granite, uncrushed river gravel and artisanal crushed granite, and analyzed the results with a stress-life regression, a two-parameter Weibull description of life scatter and a secant-modulus degradation model.

The fitted stress-life slopes of 16.732, 16.460 and 17.281 fall between the published relations of Tepfers and Kutti (1979) and Aas-Jakobsen (1970), which places these results inside established practice. On the ordering measured here, the design consequence is large and it inverts under the change of basis. River gravel costs a factor of 7.47 in mean fatigue life at a design stress ratio of 0.65 and 18.08 in characteristic life at five percent failure probability. Artisanal granite costs only 3.48 on the mean but 22.09 on the characteristic basis, so the material that looks better on average is the worse choice for design. Stiffness degradation follows the established three-stage form for all three sources, with retained moduli at failure of 0.651, 0.556 and 0.599, and separates them weakly.

The result we would emphasize concerns detection rather than magnitude. With the artisanal supply carrying the coefficient of variation that published quality-control data attaches to uncontrolled production, an analysis of variance on 28-day compressive strength across the three materials returned $F(2,33) = 3.27$ and $p = 0.051$, and Tukey's procedure could not separate commercial from artisanal granite at all. Three materials whose characteristic fatigue lives differ by more than a factor of twenty are indistinguishable under the acceptance test that Nigerian practice actually applies. The analytical counterpart is that for Weibull-distributed life the ratio of characteristic to mean life is fixed by the shape parameter alone, falling from 0.131 at $\alpha = 1.396$ to 0.021 at $\alpha = 0.792$.

We therefore recommend that aggregate acceptance for repeatedly loaded concrete constrain the dispersion of the supply and not only its mean, that source approval for fatigue-critical elements be granted per quarry rather than per rock type, and that where a variable source is unavoidable the design stress ratio be reduced rather than the material rejected, since a slab thickness increase of the order of ten percent recovers a factor of 53 in characteristic life for the weakest case examined.

The test program and the analysis are documented here in enough detail to be repeated, and a wider study drawing on more quarries across Osun State would show how far these three sources represent the supply. Any repeat should use more than twelve specimens per stress level, since twelve does not resolve the shape parameter reliably. Beyond it, extension to variable-amplitude loading through a damage and fracture treatment of the kind proposed by Keerthana and Chandra Kishen (2018), and a paired study of aggregate source against site batching practice, would address the two largest remaining sources of uncertainty.

REFERENCES

[1] Aas-Jakobsen, K. 1970. *Fatigue of Concrete Beams and Columns*. Bulletin Nos. 70-1. Institutt for Betonkonstruksjoner, Norges Tekniske Høgskole (NTH).

[2] ACI Committee 214. 2002. *ACI 214R-02, Evaluation of Strength Test Results of Concrete*. American Concrete Institute, Farmington Hills, MI.

[3] Ajagbe, W. O., M. A. Tijani, and O. A. Agbede. 2018. "Compressive Strength of Concrete Made from Aggregates of Different Sources." *USEP Journal of Research Information in Civil Engineering (JRICE)* 15 (1): 1963–74.

[4] Ajagbe, W. O., M. A. Tijani, and I. A. Oyediran. 2015. "Engineering and Geological Evaluation of Rocks for Concrete Production." *LAUTECH Journal of Engineering and Technology* 9 (2): 67–79.

[5] American Concrete Institute. 1992. *ACI 215R-92 (Reapproved 1997), Considerations for Design of Concrete Structures Subjected to Fatigue Loading*. American Concrete Institute.

[6] Aslani, Farhad, and Raha Jowkarmeimandi. 2012. "Stress–Strain Model for Concrete Under Cyclic Loading." *Magazine of Concrete Research* 64 (8): 673–85. https://doi.org/10.1680/macr.11.00120.

[7] ASTM International. 2014. *ASTM C469/C469M-14e1, Standard Test Method for Static Modulus of Elasticity and Poisson's Ratio of Concrete in Compression*. ASTM International.

[8] Bamigboye, G. O., A. N. Ede, U. E. Umana, T. O. Odewumi, and O. A. Oluwu. 2016. "Assessment of Strength Characteristics of Concrete Made from Locally Sourced Gravel from South-South Nigeria." *British Journal of Applied Science & Technology* 12 (5): 1–10.

[9] Bamigboye, G. O., D. O. Olukanni, A. A. Adedeji, B. U. Ngene, K. J. Jolayemi, and A. Ajao. 2018. "Physical and Mechanical Properties of Concrete Made with Local Gravel for Sustainable Construction: Case Study Ogun and Oyo States, Nigeria." *International Journal of Civil Engineering and Technology (IJCIET)* 9 (11): 2978–85.

[10] Beushausen, Hans, and Thomas Dittmer. 2015. "The Influence of Aggregate Type on the Strength and Elastic Modulus of High Strength Concrete." *Construction and Building Materials* 74: 132–39. https://doi.org/10.1016/j.conbuildmat.2014.08.055.

[11] Breccolotti, Marco, Massimo Federico Bonfigli, Antonella D'Alessandro, and Annibale Luigi Materazzi. 2015. "Constitutive Modeling of Plain Concrete Subjected to Cyclic Uniaxial Compressive Loading." *Construction and Building Materials* 94: 172–80. https://doi.org/10.1016/j.conbuildmat.2015.06.067.

[12] British Standards Institution. 1989. *BS 812-105.1:1989, Testing Aggregates – Part 105: Methods for Determination of Particle Shape, Section 105.1 Flakiness Index*. British Standards Institution.

[13] British Standards Institution. 1990a. *BS 812-110:1990, Testing Aggregates – Part 110:*

Methods for Determination of Aggregate Crushing Value (ACV). British Standards Institution.

[14] British Standards Institution. 1990b. *BS 812-112:1990, Testing Aggregates – Part 112: Method for Determination of Aggregate Impact Value (AIV)*. British Standards Institution.

[15] British Standards Institution. 1997. *BS 8110-1:1997, Structural Use of Concrete – Part 1: Code of Practice for Design and Construction*. British Standards Institution.

[16] British Standards Institution. 2009a. *BS EN 12390-3:2009, Testing Hardened Concrete – Part 3: Compressive Strength of Test Specimens*. British Standards Institution.

[17] British Standards Institution. 2009b. *BS EN 12390-5:2009, Testing Hardened Concrete – Part 5: Flexural Strength of Test Specimens*. British Standards Institution.

[18] Cachim, P. B., J. A. Figueiras, and P. A. A. Pereira. 2002. "Fatigue Behavior of Fiber-Reinforced Concrete in Compression." *Cement and Concrete Composites* 24 (2): 211–17. https://doi.org/10.1016/S0958-9465(01)00019-1.

[19] Chen, Xudong, Jingwu Bu, Xueqian Fan, Jianyong Lu, and Liang Xu. 2017. "Effect of Loading Frequency and Stress Level on Low Cycle Fatigue Behavior of Plain Concrete in Direct Tension." *Construction and Building Materials* 133: 367–75. https://doi.org/10.1016/j.conbuildmat.2016.12.085.

[20] Gaedicke, Cristian, Jeffery Roesler, and Surendra Shah. 2009. "Fatigue Crack Growth Prediction in Concrete Slabs." *International Journal of Fatigue* 31 (8-9): 1309–17. https://doi.org/10.1016/j.ijfatigue.2009.02.040.

[21] Goel, S., and S. P. Singh. 2014. "Fatigue Performance of Plain and Steel Fibre Reinforced Self-Compacting Concrete Using s–n Relationship." *Engineering Structures* 74: 65–73. https://doi.org/10.1016/j.engstruct.2014.05.010.

[22] International Federation for Structural Concrete (fib), ed. 2013. *Fib Model Code for Concrete Structures 2010*. Ernst & Sohn (Wiley). https://doi.org/10.1002/9783433604090.

[23] Isojeh, Benard, Maria El-Zeghayar, and Frank J. Vecchio. 2017. "Concrete Damage Under Fatigue Loading in Uniaxial Compression." *ACI Materials Journal* 114 (2): 225–35. https://doi.org/10.14359/51689477.

[24] Joshua, O., O. I. Fagbenle, K. O. Olusola, et al. 2018. "A Comparative Analysis of Batching by Weight and Volume Towards Improved Concrete Production." *Construction Research Congress 2018*, 582–91. https://doi.org/10.1061/9780784481295.058.

[25] Keerthana, K., and J. M. Chandra Kishen. 2018. "An Experimental and Analytical Study on Fatigue Damage in Concrete Under Variable Amplitude Loading." *International Journal of Fatigue* 111: 278–88. https://doi.org/10.1016/j.ijfatigue.2018.02.014.

[26] Kim, Sunghwan, Halil Ceylan, Di Ma, and Kasthurirangan Gopalakrishnan. 2014. "Calibration of Pavement ME Design and Mechanistic-Empirical Pavement Design Guide Performance Prediction Models for Iowa Pavement Systems." *Journal of Transportation Engineering* 140 (10): 04014052. https://doi.org/10.1061/(asce)te.1943-5436.0000704.

[27] Lantsoght, Eva O. L., Cornelis van der Veen, and Ane de Boer. 2016. "Proposal for the Fatigue Strength of Concrete Under Cycles of Compression." *Construction and Building Materials* 107: 138–56. https://doi.org/10.1016/j.conbuildmat.2016.01.007.

[28] Lee, M. K., and B. I. G. Barr. 2004. "An Overview of the Fatigue Behaviour of Plain and Fibre Reinforced Concrete." *Cement and Concrete Composites* 26 (4): 299–305. https://doi.org/10.1016/S0958-9465(02)00139-7.

[29] Maximos, Hany, Ece Erdogmus, and Maher K. Tadros. 2010. "Fatigue Evaluation for Reinforced Concrete Box Culverts." *ACI Structural Journal* 107 (1): 13–20. https://doi.org/10.14359/51663384.

[30] Medeiros, A., X. Zhang, G. Ruiz, Rena C. Yu, and M. S. L. Velasco. 2015. "Effect of the Loading Frequency on the Compressive Fatigue Behavior of Plain and Fiber Reinforced Concrete." *International Journal of Fatigue* 70: 342–50. https://doi.org/10.1016/j.ijfatigue.2014.08.005.

[31] Nduka, David O., Olabosipo I. Fagbenle, Opeyemi Joshua, Ayodeji O. Ogunde, and Ignatius O. Omuh. 2018. "Comparative Analysis of Concrete Strength Utilizing Quarry-Crushed and Locally Sourced Coarse Aggregates." *International Journal of Mechanical Engineering and Technology (IJMET)* 9 (1): 609–17.

[32] Oh, Byung Hwan. 1986. "Fatigue Analysis of Plain Concrete in Flexure." *Journal of Structural Engineering (ASCE)* 112 (2): 273–88. https://doi.org/10.1061/(ASCE)0733-9445(1986)112:2(273).

[33] Oh, Byung Hwan. 1991. "Fatigue-Life Distributions of Concrete for Various Stress Levels." *ACI Materials Journal* 88 (2): 122–28.

[34] Olonade, K. A., I. K. Ajibola, and C. L. Okeke. 2018. "Performance Evaluation of Concrete Made with Sands from Selected Locations in Osun State, Nigeria." *Case Studies in Construction Materials* 8: 160–71. https://doi.org/10.1016/j.cscm.2018.01.004.

[35] Olutaiwo, A. O., A. A. Ashamo, and A. Adanikin. 2018. "Mechanical Strength Determination of Crushed Stone Aggregate Fraction for Road Pavement Construction (Case Study: Selected Quarries in Western Nigeria)." *Proceedings of the FUOYE First International Engineering Conference (FICE 2018)* (Ikole-Ekiti, Nigeria).

[36] Oneschkow, Nadja. 2016. "Fatigue Behaviour of High-Strength Concrete with Respect to Strain and Stiffness." *International Journal of Fatigue* 87: 38–49. https://doi.org/10.1016/j.ijfatigue.2016.01.008.

[37] Packard, Robert G., and Shiraz D. Tayabji. 1984. *Thickness Design for Concrete Highway and Street Pavements*. Engineering Bulletin EB109.01P. Portland Cement Association.

[38] Plei, Michael, and Shiraz D. Tayabji. 2012. *Continuously Reinforced Concrete Pavement Performance and Best Practices*. ACPT TechBrief FHWA-HIF-12-039. Federal Highway Administration, Office of Pavement Technology.

[39] Ponnada, Markandeya Raju. 2014. "Combined Effect of Flaky and Elongated Aggregates on Strength and Workability of Concrete." *International Journal of Structural Engineering* 5 (4): 314–25. https://doi.org/10.1504/IJSTRUCTE.2014.065915.

[40] Sachs, Steven, Julie M. Vandenbossche, and Mark B. Snyder. 2015. "Calibration of National Rigid Pavement Performance Models for the Pavement Mechanistic–Empirical Design Guide." *Transportation Research Record* 2524 (1): 59–67. https://doi.org/10.3141/2524-06.

[41] Santos, Antônio Carlos dos, Angela Maria de Arruda, Turibio José da Silva, Paula de Carvalho Palma Vitor, and Leandro Mouta Trautwein. 2017. "Influence of Coarse Aggregate on Concrete's Elasticity Modulus." *Acta Scientiarum. Technology* 39 (1): 17–25. https://doi.org/10.4025/actascitechnol.v39i1.29873.

[42] Saucedo, L., Rena C. Yu, A. Medeiros, X. Zhang, and G. Ruiz. 2013. "A Probabilistic Fatigue Model Based on the Initial Distribution to Consider Frequency Effect in Plain and Fiber Reinforced Concrete." *International Journal of Fatigue* 48: 308–18. https://doi.org/10.1016/j.ijfatigue.2012.11.013.

[43] Sriram, V., Konakanchi Sirisha, R. Keerthi Prakash, G. Murali, M. K. Haridharan, and K. Karthikeyan. 2017. "A New Method to Estimate Weibull Parameter for the Fatigue Life of Self Compacting Fibre Reinforced Concrete Beams." *International Journal of Civil Engineering and Technology (IJCIET)* 8 (7): 326–31.

[44] Sulymon, N., O. Ofuyatan, O. Adeoye, et al. 2017. "Engineering Properties of Concrete Made from Gravel Obtained in South-West Nigeria." *Cogent Engineering* 4: 1295793. https://doi.org/10.1080/23311916.2017.1295793.

[45] Tepfers, Ralejs, and Tom Kutti. 1979. "Fatigue Strength of Plain, Ordinary, and Lightweight Concrete." *ACI Journal Proceedings* 76 (5): 635–52.

[46] Tsado, Theophilus Yisa. 2013. "A Comparative Analysis of Concrete Strength Using Igneous, Sedimentary and Metamorphic Rocks (Crushed Granite, Limestone and Marble Stone) as Coarse Aggregate." *International Journal of Engineering Research & Technology (IJERT)* 2 (9).

[47] Vishalakshi, K. P., V. Revathi, and S. Sivamurthy Reddy. 2018. "Effect of Type of Coarse Aggregate on the Strength Properties and Fracture Energy of Normal and High Strength Concrete." *Engineering Fracture Mechanics* 194: 52–60. https://doi.org/10.1016/j.engfracmech.2018.02.029.

[48] Zanuy, Carlos, Luis Albajar, and Pablo de la Fuente. 2011. "The Fatigue Process of Concrete and Its Structural Influence." *Materiales de Construcción* 61 (303): 385–99. https://doi.org/10.3989/mc.2010.54609.